Performance of MoS_2 Coated Gears Exposed to Humid Air During Storage

Timothy Krantz*, Claef Hakun**, Zachary Cameron*, Iqbal Shareef+, Michael Dube++

Abstract

The purpose of this work was to study the effect of exposure to humid air on the durability of a molybdenum disulfide (MoS_2) dry film lubricant on spur gears operated in vacuum. This study was motivated by the James Webb Space Telescope (JWST) Mission. Some mechanisms of the JWST using MoS_2 dry film lubricants have been exposed to humid air during storage as a subassembly and after integration into a higher-level assembly. In this study MoS_2 dry film lubricant was applied to steel spur test gears and subsequently tested in vacuum environment. One-half of the gears had essentially zero time exposure to humid air prior to testing, and the other half were exposed to humid air of 57 percent relative humidity up to 77 days prior to testing. All tests were completed at constant torque and speed. On average the film durability was shorter for gears exposed to humid air compared to those with zero exposure. For the unexposed gears, the durability ranged from 53,300 to 190,300 pinion revolutions with an average value of 100,200 and a median value of 83,500 revolutions. For the exposed gears, the durability ranged from 21,000 to 84,700 pinion revolutions with an average value of 64,900 and a median value of 68,800 revolutions. Using the unexposed gears as a baseline, the exposure reduced the average durability by 35 percent and the median value of durability by 18 percent. Red-brown coloration was noted on some of the gear teeth that had been exposed to humid air. The colored regions appeared as soon as 17 days after exposure to humid air. SEM inspections showed that at least some of these colored areas included material raised above the surrounding MoS_2 film.

Introduction

The purpose of this work was to study the effect of exposure to humid air on the durability of a molybdenum disulfide (MoS_2) dry film lubricant on spur gears operated in vacuum.

This study was motivated by the James Webb Space Telescope (JWST) Mission, and the study is one part of a NASA Engineering Safety Center effort to evaluate potential risks and performance effects to JWST instrument mechanisms and components lubricated with sputtered MoS_2 coatings. The coatings are exposed to humid air environments during integration, ground operations, and storage prior to launch. The mechanism configurations included in the scope of the study are the fine guidance sensor (FGS) course focus mechanism, the FGS fine focus mechanism, the FGS dual-wheel mechanism, and the near-infrared camera focus adjust mechanism. Some details about the design, life testing, and engineering enhancements of these mechanisms have been reported [1-3]. The mentioned mechanisms have sputtered MoS_2 dry film lubricants on gears and other components. The practical effects of exposure to humidity on the performance of MoS_2 are not fully understood, and to our knowledge a dedicated study of such effects have not been conducted for MoS_2 films lubricating gear teeth. The focus of this study was the durability of a MoS_2 dry film lubricant on spur test gears that have been exposed to humid air up to 77 days..

* NASA Glenn Research Center, Cleveland, OH
** NASA Goddard Space Flight Center, Greenbelt MD
+ Bradley University, Peoria, IL
++ NASA Langley Research Center (NESC), Hampton, VA

Proceedings of the 44th Aerospace Mechanisms Symposium, NASA Glenn Research Center, May 16-18, 2016

Lince, Loewenthal, and Clark provide a recent and thorough discussion of previous studies regarding MoS_2 aging and oxidation. They comment that long-term storage life test data for sputter-deposited MoS_2 coatings are uncommon [4]. They also completed and reported a study, motivated by the JWST observatory, on the degradation of three nanocomposite MoS_2 coatings during storage in air. The tests used to evaluate endurance were pin-on-disk tests, and storage times were up to 2.3 years. They found that exposure to air could degrade the endurance of the coatings by up to 55 percent. The severity of degradation depended on both the exposure duration and coating composition.

Experimental Equipment

Test Gears

Readily available stock gears with appropriate center distance were selected and customized for use in this study. The customizations of the stock gear design were the bore diameters, sized for a commercial off-the-shelf keyless shaft-locking device, and custom face widths. The pinions and gears were 3mm module spur gears with standard tooth proportions. The pinions had 26 teeth and a 13 mm face width. The gears had 48 teeth and 10 mm face width. There were six pairs of pinions and gears. The material was S45C steel (equivalent to AISI 1045). The teeth were induction hardened to surface hardness of HRc 50-60 and ground.

The test gears were coated with MoS_2 by sputtering. While certain mechanisms of the JWST use nanocomposite MoS_2 coatings [4], the mechanisms of interest for this work have a pure MoS_2 coating, and so the test gears were provided with such a composition. The chamber capacity required two coating runs. Witness coupons were in the chamber during sputtering. The thickness of the coating on the witness coupons were reported by the vendor to be 37,000 angstroms for one run and 30,000 angstroms for the second run. After coating the test gears were sealed in bags using a dry inert cover gas by the coating vendor. Gears to be tested as unexposed remained in the sealed bags until the start of the installation procedure. The time from the opening of the bag until the gears were in a vacuum condition in the gear test rig was minimized to all practical extent.

The tooth surface roughness was measured along the involute profile direction of a randomly selected pinion tooth using a stylus profilometer prior to sputtering. Another tooth was inspected after sputtering and subsequent exposure to humid air prior to testing. The data were filtered using an ISO standard Gaussian filter with 0.8 mm cutoff and 300:1 bandwidth. The resulting calculated roughness average value, 0.42 micrometer Ra, was the same prior to and after sputtering. The peak-to-valley range of the roughness-filtered data was approximately the same as the measured thickness of the coating on witness samples that were in the sputtering chamber with the gears. The roughness topography features were the same prior to and after sputtering (Fig. 1).

One half of the available tooth surfaces were exposed to humid air prior to testing. The exposure was done in a closed chamber with the gears placed on a perforated plate. Beneath the plate was a saturated solution of water and sodium bromide. The saturated salt solution provided a relative humidity of approximately 57 percent, this value being near the upper limit 60 percent relative humidity of certain storage conditions for the mechanisms of interest.

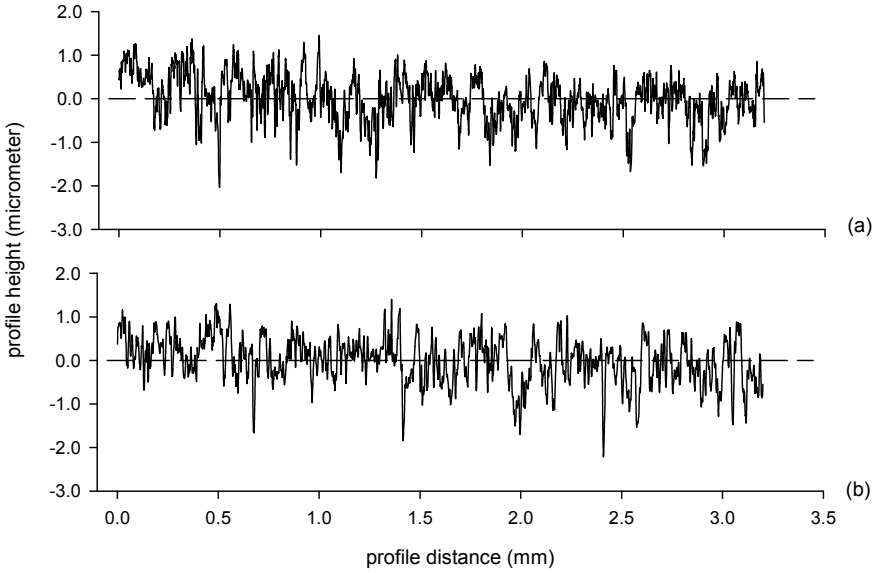

Figure 1 – Roughness profiles of pinion teeth, measurement along the involute direction. (a) Prior to sputtering. (b) After sputtering and then exposure to humid air.

Gear Test Rig

To accomplish gear testing in vacuum, a test rig previously used for testing of rollers [5-7] was adapted for gear testing. To adapt the rig, the spacing from the input to the output shaft was increased from 36 mm used for roller testing to 112 mm for gear testing. Otherwise, the rig setup was the same as had been used for roller testing.

The vacuum gear rig is depicted in schematic form in Figure 2. The pinion motion is provided by a variable speed electric motor. A magnetic-particle brake attached to the output shaft imposes torque on the gear. A pressurized air cylinder controls the pinion position. The air cylinder acts through a pivot axis to rotate the drive motor plate that mounts the driving shaft and drive motor. The rotation of the drive motor plate moves the pinion toward the gear in an arc motion to bring the teeth into mesh. The pressure to the cylinder, and thereby shaft center distance, is adjusted by a hand-operated valve. A linear variable displacement transducer (LVDT) measures the position of the drive motor plate, and this sensor output was used to establish the proper operating center distance. The rig features a turntable that is used to impose controlled misalignment of shafts for roller experiments. For gear testing, the turntable was adjusted to provide for an aligned shaft condition. A turbomolecular pump assisted by a scroll pump provides vacuum in the test chamber. Ferrofluid seals maintain the vacuum at the shaft-chamber interfaces. The typical condition in the test chamber is a pressure of 3x10-7 Torr. The most prevalent remaining constituent in the chamber during testing is water vapor as was determined using a residual gas analyzer [8].

The torque on the output shaft is measured by a strain-gage type torquemeter of 22 N-m (200 in-lb) torque capacity. Calibration was done in place using deadweights acting on a torque arm of known length attached at the test gear position and reacting the output shaft to ground.

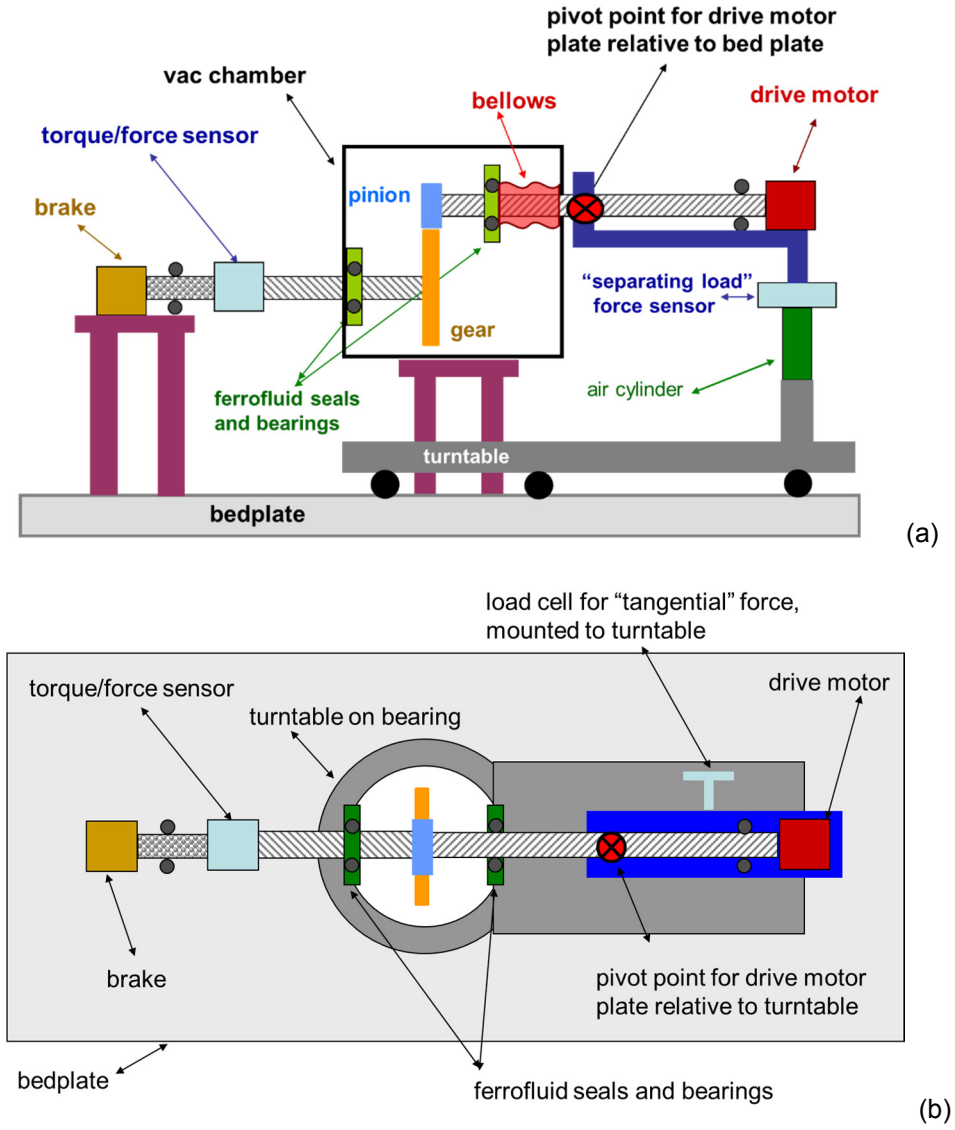

Figure 2 – Schematic representation of vacuum gear rig. (a) Side view. (b) Overhead view.

The force created by the meshing gear teeth can be described as three orthogonal forces. Each of these force components influences a sensor as will be described with the aid of Figure 2. The tooth force component directed tangent to the pitch circle is termed the tangential force. The torque on the gear is a product of the tangential force and the operating pitch radius. The gear tooth tangential force attempts to rotate the drive motor plate about a pivot axis, but the table is constrained to the turntable through a load sensor termed as the "tangential" force sensor. The tooth force component directed along the line joining the gear centers, the separating force, acts through a pivot axis and thereby attempts to tilt the drive motor table, but the table motion is constrained by the air cylinder through a sensor termed the "separating load" force sensor. Because the drive motor plate is not balanced about the pivot point, the force measured on this "separating force" sensor is a combination of the gear separating force action and the unbalanced overhung weight of the motor and plate. The third component of gear tooth force acts along the direction of the gear shaft, the gearing thrust force. Although spur gears create, theoretically, zero thrust forces, in practice a thrust force is indeed created because of inevitable manufacturing tolerances and small mounting misalignments. The magnitude of the resulting thrust force depends in part

on the friction between the mating gear teeth. The action of spur gears creating a thrust force is analogous to the friction-dependent thrust forces created by misaligned rollers (Ref. 5).

Shaft speeds and total number of shaft revolutions were measured using encoders on each shaft. The encoder pulses were counted and recorded via a digital pulse counter. The encoders provide 6,000 pulses for each shaft revolution.

A linear variable differential transformer (LVDT) measures the tilting position of the drive motor plate. The tilting of the plate changes the pinion-to-gear center distance, and so the LVDT output thereby measures the operating center distance. As the gears operate, the operating center distance changes slightly because of the gearing action. As the tooth contact position on the pinion moves from the dedendum, through the pitch point, and to the addendum region, the friction force changes direction. This changing friction force causes slight changes in the instantaneous center distance, because of elastic deflections, and thereby the friction force affects the output of the LVDT.

The gear teeth surface conditions were photographed at regular intervals during testing through a viewport. The images were captured digitally using a single-lens reflex camera with a 150 mm micro lens and a 12 million effective pixel image sensor.

Experiment Method

The experimental approach was to conduct an equal number of tests using unexposed and exposed surfaces. The test matrix of Table 1 was selected for the study. The pinions and gears were assigned randomly as 6 test pairings per Table 1. With the ability to test both front (side “A”) and back (side ”B”) of each tooth, 12 tests were possible. Test article pairings 1 through 4 were assigned to have side “A” tested with zero exposure to humid air. There was some minimal exposure time to air during installation procedure into the rig, but in this report such minimal exposure is considered as zero exposure. For test article pairings 1 through 4, once “side A” of the teeth were tested, the pair was placed into the humidity exposure chamber to begin the exposure time for the tooth sides “B”. For gear pair 5, there was zero exposure and sides “A” of the teeth were tested. Then the test chamber was opened long enough to remove the gears from the shafts and remount immediately for testing of teeth sides “B” as also unexposed. For test article pair 6, the pinion and gear were placed into the exposure chamber at the beginning of the test program to obtain a long exposure time while testing the other gears. Both sides “A” and “B” of pair 6 were tested after an exposure time of 77 days. The exposure times for other test were less than 77 days as was dictated by the testing pace and sequence.

As the test sequence progressed, it was decided that photo documentation of the conditions of the teeth prior to test may prove insightful. Beginning with the fifth test in the testing order sequence (test MoS2 4-A, per Table 1) the first step of the testing sequence was to document the visual condition of each gear by digital photographs. Next, the gear pair was then mounted onto the test shafts, the vacuum chamber closed, and then the chamber vacuum condition was established over several hours, and typically overnight, prior to applying torque and motion. The chamber pressure was 7×10^{-7} Torr or less at the beginning of each test. Figure 3 shows a pair of the MoS_2 coated test gears out of sealed bags just prior to test and in the test chamber just prior to closing the vacuum chamber door.

Table 1. Test matrix.

Test Name	Test Article Pairing	Pinion Serial Number	Gear Serial Number	Tooth Side Loaded	Exposed	Total Exposure Time (days)	Testing Order Sequence
MOS2 1-A	1	P4	G1	A	No	-	1
MOS2 1-B				B	Yes	10	3
MOS2 2-A	2	P6	G6	A	No	-	2
MOS2 2-B				B	Yes	28	6
MOS2 3-A	3	P2	G2	A	No	-	4
MOS2 3-B				B	Yes	17	9
MOS2 4-A	4	P1	G3	A	No	-	5
MOS2 4-B				B	Yes	17	10
MOS2 5-A	5	P3	G5	A	No	-	7
MOS2 5-B				B	No	-	8
MOS2 6-A	6	P5	G4	A	Yes	77	11
MOS2 6-B				B	Yes	77	12

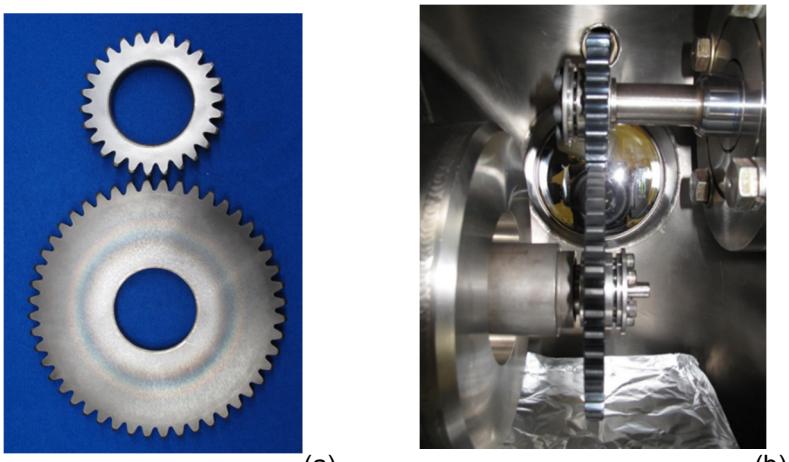

(a) (b)

Figure 3 – Test gears. (a) Just prior to testing.
(b) Installed it rig just prior to closing test chamber.

Testing was done at a constant brake torque and motor speed. The torque was 6.8 Nm for the gear as was applied by the brake and measured by torque sensor. The test speed was 80 rpm for the pinion (and consequently 43.3 rpm for the gear). The power transmitted was 31 watts. The torque was selected to provide a tooth load intensity (force per unit face width) similar to the tooth load intensity for the mechanisms of interest. The speed was selected as the maximum speed that did not induce any significant rig dynamic loading or vibrations as had been determined by previous testing of similar test gears. Testing for endurance of the coatings typically required durations longer than a working day, and unattended testing was not attempted. The testing was paused overnight, as needed, with the test chamber vacuum maintained by continuous operation of the turbopump, and then testing was resumed the following day.

The test progression was monitored by visual inspection of the tooth surfaces through a viewport, aided at times by a strobe light to “freeze” the motion. The visual condition was also recorded by digital photographs illuminated by a short duration flash through a second viewport that provided a view of the

gear teeth (but not of pinion teeth). The test progression was monitored by displays of the sensor data plotted as functions of pinion revolutions. Some previous development test revealed that as wear severity and friction increase, sensor outputs became more erratic even though their mean value remain constant. For example, when friction on the gear teeth increases, the range of the separation force increases even though the mean may still be constant. This phenomenon is the result of the tooth friction force reversing direction as the tooth contact passes through the pitch point. Thereby, the friction force first adds to, and then subtracts from, the magnitude of the separating force during the tooth mesh cycle. With higher tooth friction the excursions from the mean become larger. These observations and experience in health monitoring of geared machines led to the definition and use of "condition indicators" as a means to monitor the overall capability of the MoS_2 films to provide low friction. Condition indicators were defined as follows. Data records were collected for 1 second at 1 kHz sampling rate. For each data record, the standard deviation was calculated as the "condition indicator", stored, and plotted as a function of accumulated pinion revolutions. Such condition indicators were reliable indicators of a change in the MoS_2 performance. Figure 4(a) provides a trend plot from test MOS2 1B of the condition indicator for the LVDT sensor that measures gear center distance changes. Marked on the plot is the indication where the MoS_2 functioning compromise has started. Also marked are three regions: Region I being the smooth running regime, Region II being near the start of MoS_2 compromise, and Region III being a significant friction regime. An example of a data record from which a "condition indicator" was calculated is shown in Figure 4(b), for the thrust force sensor, during operation in Region III. In plot of 4(b) there was relatively high tooth friction during the last 400 samples of this particular data record causing a varying thrust force.

Film durability was determined using the condition indicator trend plots. The film durability was defined as the number of pinion revolutions until the film compromise started, such as indicated on Figure 4. The film compromise was defined as the very beginning of a steady degradation of the film's performance regarding friction. A mechanism may continue to perform its intended function for some time after such film degradation begins. The intent was to assess a relative measure of the film durability, with and without exposure to humid air.

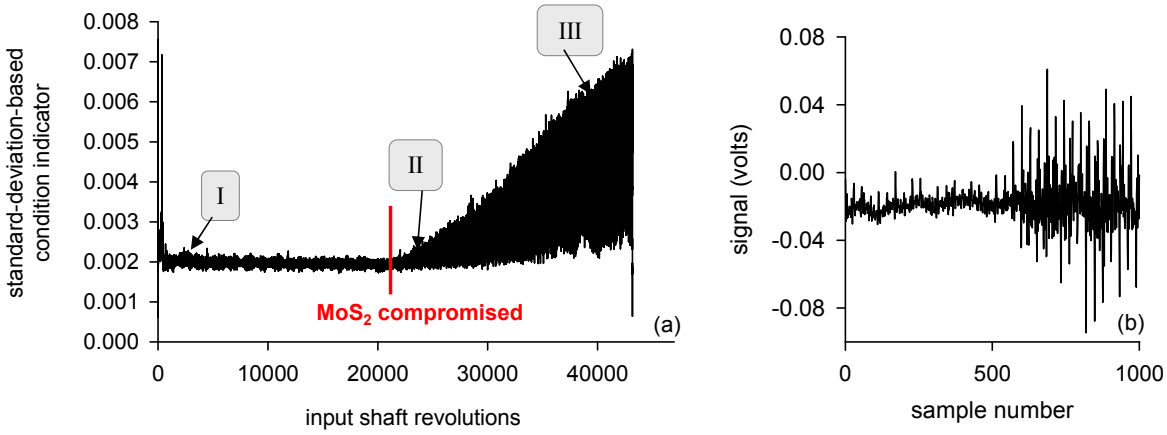

Figure 4 – Typical trend and features of a condition indicator of MoS_2 film function. (a) Trend of condition indicator for the center distance (LVDT sensor), for test 1B. (b) Typical data record for calculation of standard-deviation-based condition indicator.

Experiment Results

First will be discussed the results of quantitative measures of film durability. As was described in the previous section, "condition indicators" were calculated from sensor data. A set of condition indicators were calculated every second. Figure 4(a) is an example condition indicator data trend plot from test 1B. The number of pinion revolutions corresponding to the start of film compromise, as marked on Figure 4, was determined for each test by visual inspection of such trend plots. This film durability measure was

determined from each of three sensors, the gear center distance, the gear thrust force, and the gear tangent force sensors. For each test, the average film durability was calculated as the average of the values from each sensor. The results are collected in Table 2. On average the film durability was shorter for gears exposed to humid air compared to gears with zero exposure. The film durability for gears with zero exposure ranged from 190,300 to 53,300 pinion revolutions with an average value of 100,200 and a median value of 83,500 revolutions. The film durability for gears exposed to humid air ranged from 84,700 to 21,000 pinion revolutions with an average value of 64,900 and a median value of 68,800 revolutions. Using the unexposed-gear film durability as a baseline, the exposure reduced the film durability by 35 percent based on average values or 18 percent based on median values. These reductions in film durability are similar magnitude compared to the 55 percent to 20 percent range of reductions reported by Lince, Loewenthal, and Clark [4].

Table 2 – Test Results of Film Durability

		Film Durability (pinion revolutions)			
Test Name	Exposure (days)	Center Distance	Thrust Force	Tangent Force	Average Value *
MOS2 1-A	0	52,000	52,000	56,000	53,333
MOS2 2-A	0	59,000	61,000	65,000	61,667
MOS2 3-A	0	207,000	184,000	180,000	190,333
MOS2 4-A	0	86,000	69,000	94,000	83,000
MOS2 5-A	0	125,000	125,000	136,000	128,667
MOS2 5-B	0	83,000	80,000	89,000	84,000
MOS2 1-B	10	21,000	20,000	22,000	21,000
MOS2 2-B	28	69,000	55,000	74,000	66,000
MOS2 3-B	17	59,000	65,000	66,000	63,333
MOS2 4-B	17	81,000	78,000	95,000	84,667
MOS2 6-A	77	84,000	76,000	88,000	82,667
MOS2 6-B	77	70,000	71,000	74,000	71,667

* average value is the average of the 3 colums to the left

unexposed group	average = 100,200	median = 83,500
exposed group	average = 64,900	median = 68,800
percent reduction	35%	18%

The film durability values, from the “Average Value” column of Table 2, are plotted as a function of the duration of exposure to humid air in Figure 5. The plot shows that while as a group the durability was longest for zero days of exposure, there is no clear trend of rate of reduction with exposure time. The range of scatter for the film durability for six tests at zero time of exposure is greater than is the difference between average durability of exposed and unexposed gears.

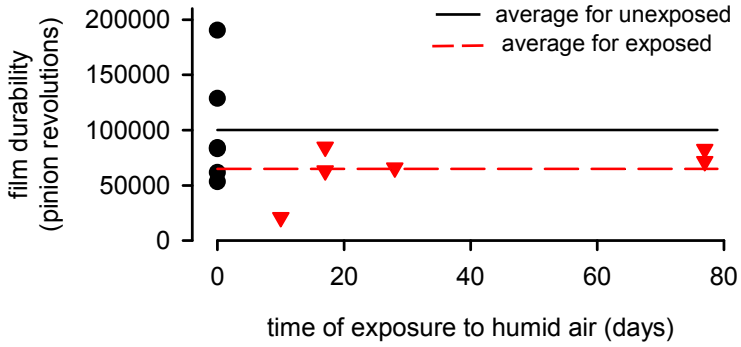

Figure 5 – Film durability as function of time of exposure to humid air.

The behaviors of the films were also evaluated by studying photographs, profilometery, and scanning electron microscope inspections. During initial running of each gear pair, it was noted that the tooth surface running-in required very few tooth contact cycles. In other words, the tooth surface appearance changed dramatically, becoming more glossy and reflective in appearance, after only a few revolutions, and subsequent further visual changes to the tooth surfaces occurred at a very slow and steady rate. Figure 6 illustrates typical results of how the surface visual appearance changed for the gear teeth during a test. The first two images from left to right show the teeth prior to any running and then again after only 1 percent of the total running time. The other two images of Fig. 6 shows the teeth after 50 percent and 99 percent of the test duration. The last two images show that with further running the visual condition changes less dramatically over the final 98 percent of running as compared to the first 1 percent of running durations.

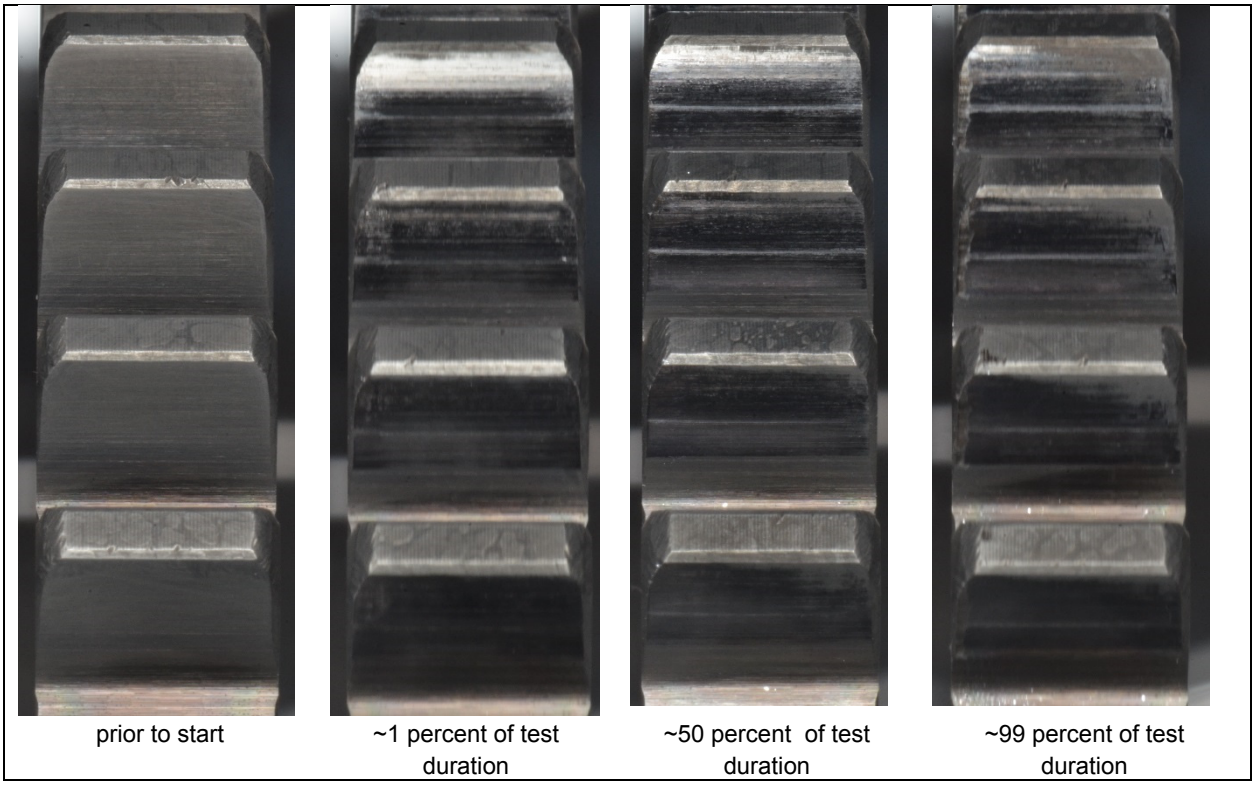

Figure 6– Gear teeth surface appearance for different durations of testing

Wear and running-in of pinion teeth were assessed using a stylus profilometer. The teeth were inspected moving the stylus with a 2-micrometer radius conisphere tip across the face width. Because the mating gear tooth face width was slightly less than that of the pinion, there were regions of the pinion tooth near each edge that did not experience contact with the gear. The data were processed to remove a least-squares linear form, using only the small regions from each edge of the trace that did not experience contact for the form removal. Traces of teeth prior to test were collected and processed in the same manner. Typical results of the inspections are provided in Figure 7. The data plots of Figs. 7(a-b) are for teeth prior to test. The surfaces show some waviness and some peak and valley features, with peak to valley distances on order of 3 micrometer, similar distance as the requested film thickness. The data plots of Figs. 7(c-d) are for tested teeth, and there is an overall wear depth of about 2 micrometer. Certain worn regions are very smooth.

After 77 days of exposure to humid air, small areas of reddish-brown coloration were noted on some teeth. Figure 8 is an example of the noted colorations. Close study of digital photographs of the pinions and gears recorded prior to testing revealed that some coloration appeared as early as 17 days after

exposure to humidity. However, not all teeth had such colored spots. For the pinion and gear pair exposed for 77 days, there was more coloration on the gear than there was on the pinion. Teeth with colorations were inspected using a scanning electron microscope (SEM). SEM images from a region having coloration, at three increasing levels of magnification, are provided in Figure 9. The image orientation has the face width direction in the vertical direction. The vertical lines are topography resulting from grinding of the teeth. This region inspected by SEM revealed that the colored areas included raised material above the surrounding surface. The highest magnification image reveals details suggesting a "growth" pushing aside and/or through the film. Figure 10(a) provides another SEM image of a similar structure as that of Fig. 9(c), from a slightly different viewpoint. During this inspection, energy-dispersive spectroscopy (EDS) was done at the four locations as marked on Fig. 10(a). The resulting spectrum of Fig. 10(b) is typical of all four inspections. The two prominent peaks of the spectrum are associated with Mo (molybdenum), S (Sulphur), and Fe (iron). It is speculated that iron oxidation was occurring at the MoS_2 film-substrate interface and progressed to eventually become evident at the surface.

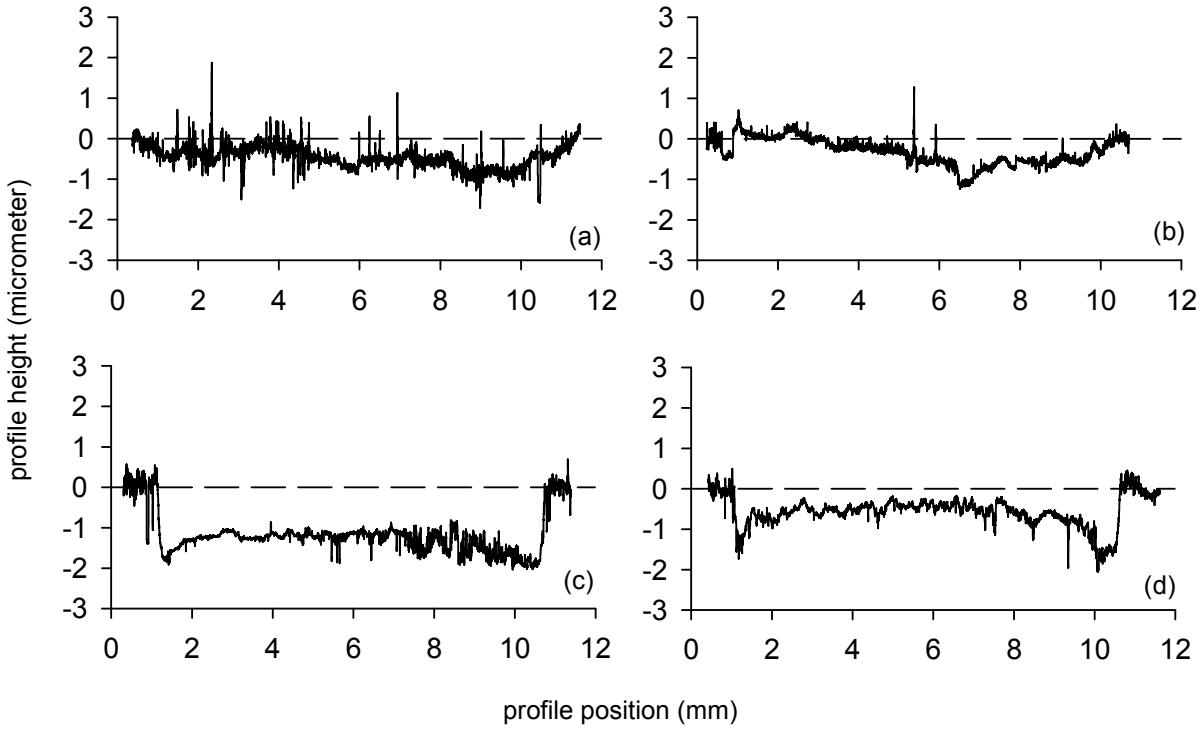

Figure 7 – Profilometer inspections of pinion teeth with traces along the face width direction. (a-b) Prior to test (c-d) After test.

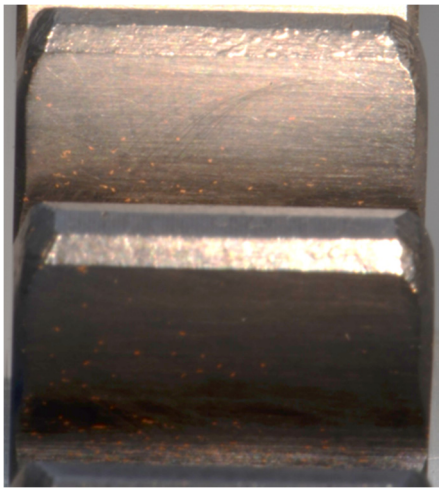

Figure 8 – Red-brown coloration noted after 77 days exposure to humid air

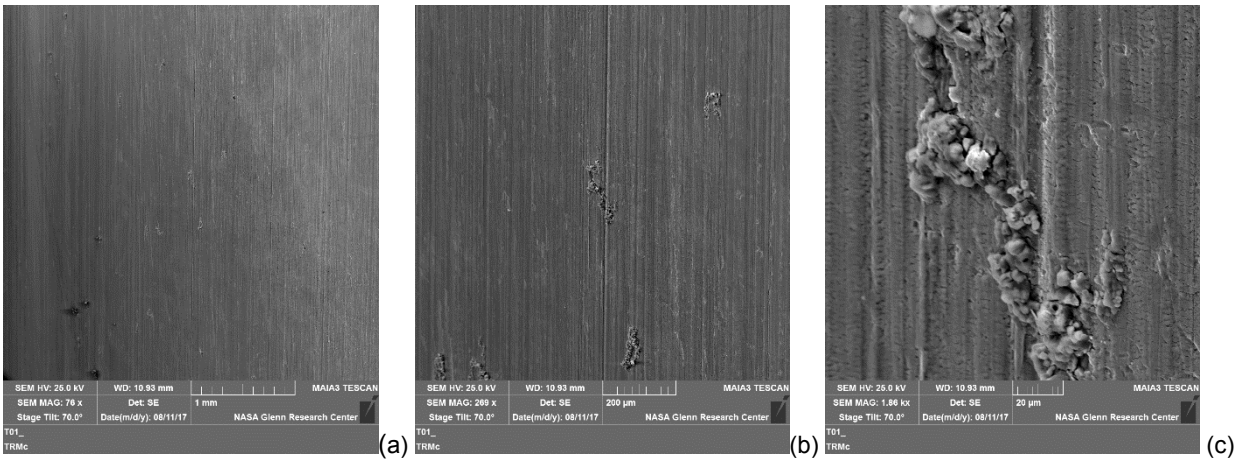

(a) (b) (c)

Figure 9 – Scanning electron microscope inspections of a region having red-brown coloration at three increasing levels of magnification. The vertical direction is the face width direction.

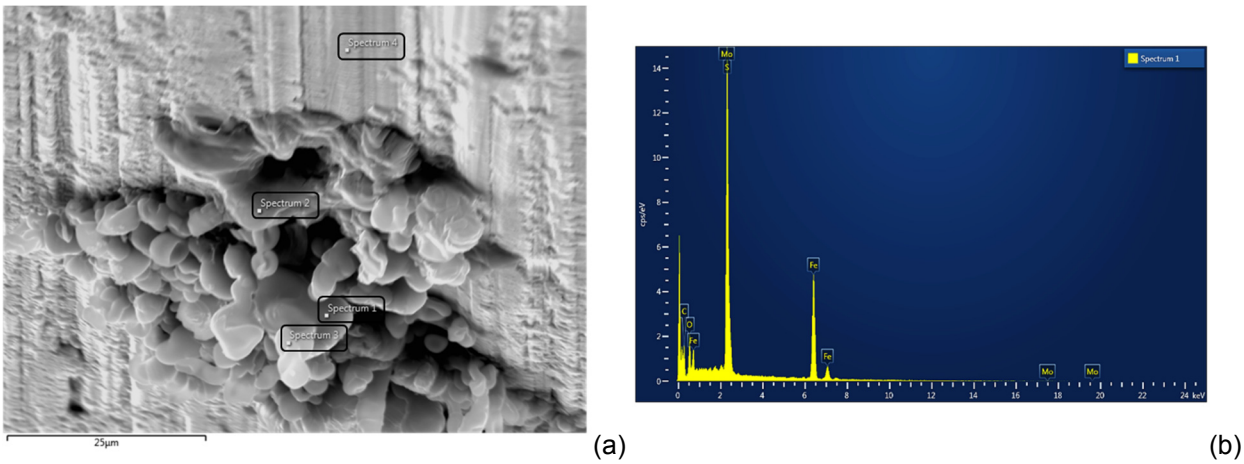

(a) (b)

Figure 10. – Scanning electron microscope inspection using energy-dispersive spectroscopy. (a) Regions inspected, per markings. (b) Spectrum for region 1, typical of all four inspections.

Study of plots of profilometry inspections of teeth prior to test revealed one inspection with an interesting topography that suggests a fortuitous tracing over a region such as revealed in the SEM images of Figs. 9(c) and 10(b). The profilometery data of this inspection, plotted using three different aspect ratios, are provided in Figure 11. The inspection was of pinon P5, in the face width direction, tooth side “B” that later was subjected to test MOS2 6B per Table 1. Fig. 11(a) reveals a localized valley feature of about 1.5 micrometer depth but having a prominent peak feature rising above, out of the valley, by about 6 micrometer. Figure 11(b) plotted using aspect-ratio 20:1 shows some details of the shape of the feature, while Fig. 11(c) illustrates the shape with true aspect ratio. The breadth of this feature is about 1.5 mm.

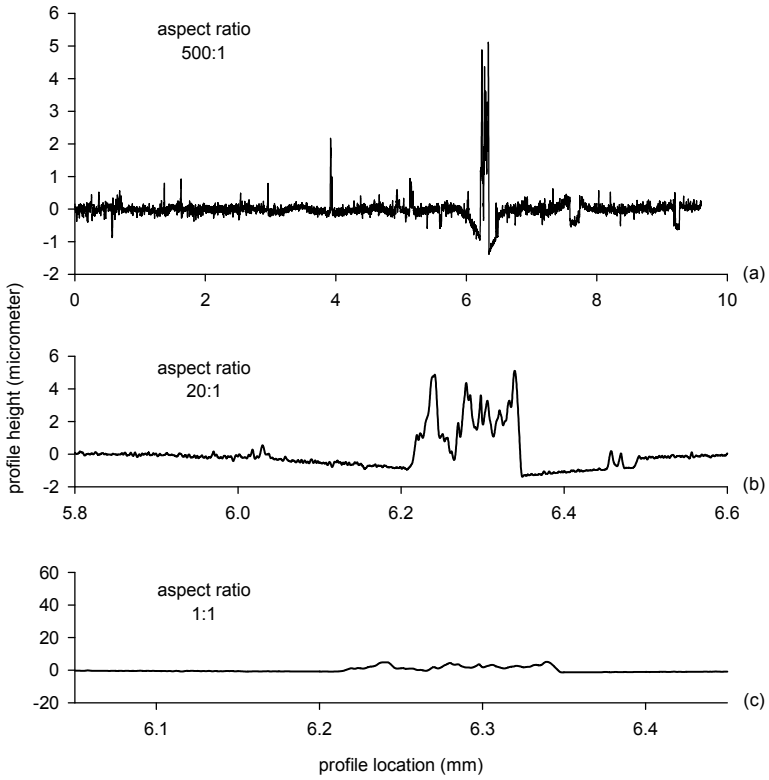

Figure 11 – Profilometer inspection of a tooth after exposure to humidity for 77 days, prior to test. The same data are plotted using three aspect ratios (500:1, 20:1 and 1:1).

SEM inspection of a tooth of the pinion, after test MOS2 2A per Table 1, revealed a wide variety of features on the worn tooth surface. An inspection summary is provide in Figure 12. Figs. 12(a) and (b) can be used to locate the features of Fig. 12(c) showing highly smoothed MoS_2, blistering, and a region of loss of film thickness that thereby revealed the underlying grinding-line striation topography. The elongated blister features are aligned with the direction of rolling and sliding. Although the “delaminated” region of Fig 12(c) might suggest exposure of the steel substrate, the higher magnified image of 12(d) has appearance of material flowing in the direction of rolling and sliding. EDS inspection near the center of this region resulted in a spectrum associated with Mo (molybdenum), S (Sulphur), and Fe (iron) showing that the region did not experience complete loss of all MoS_2 thickness through this region.

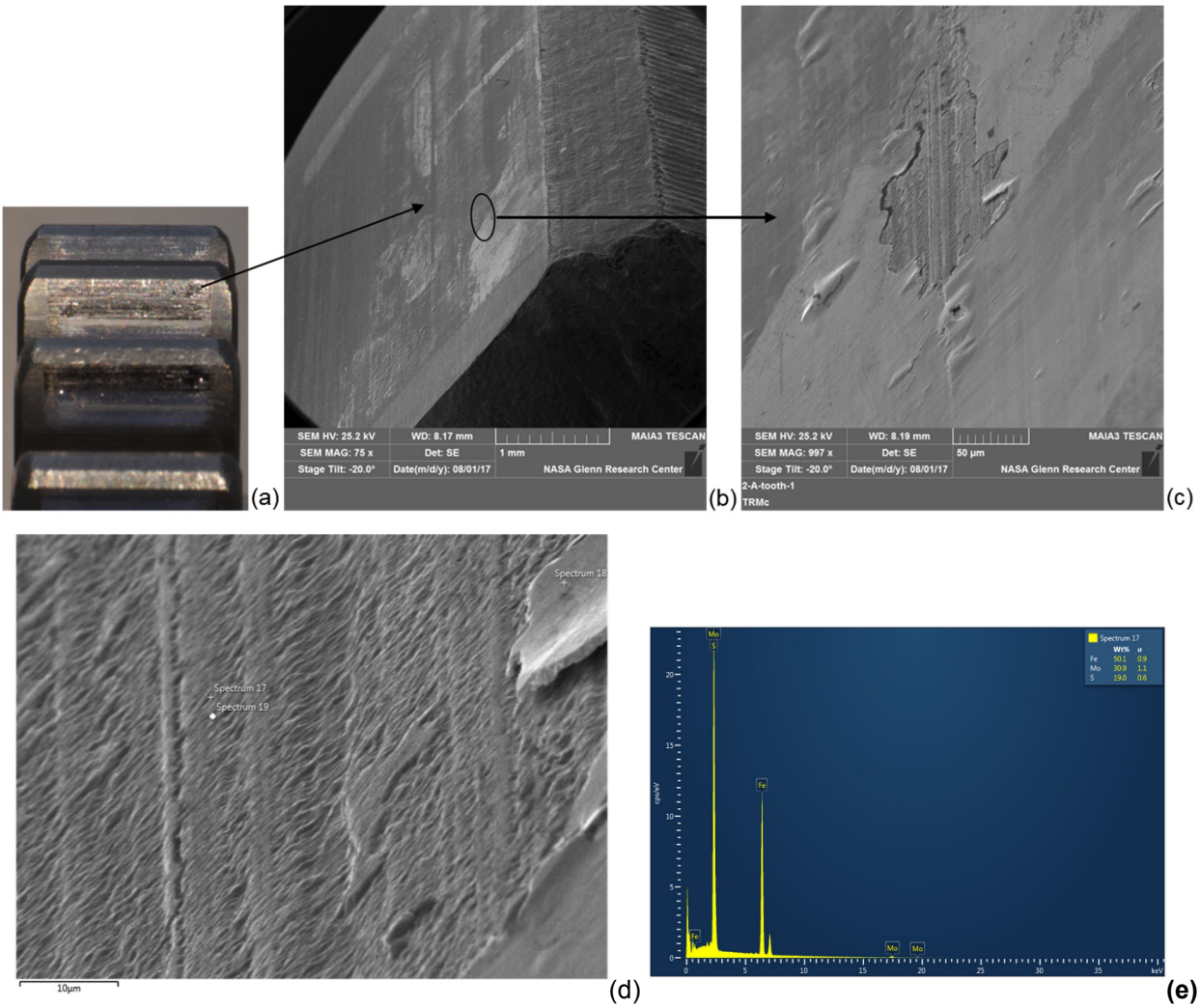

Figure 12 – Scanning electron microscope inspection summary of a pinion tooth after test 2A, no exposure to humidity prior to testing. (a) Optical image showing location of SEM inspection. (b) SEM image near tooth tip. (c) SEM image of blistering and delamination of the film. (d) Close up of delaminated region. (e) EDS spectrum taken from the center of the image immediately to left.

Summary

The purpose of this work was to study the effect of exposure to humid air on the durability of a molybdenum disulfide (MoS_2) dry film lubricant applied to spur test gears and subsequently tested in vacuum environment. MoS_2 was applied by sputtering onto gears made from induction hardened and ground S45C steel. Twelve gear tests were completed in a vacuum gear rig at constant speed and torque. For this study, film durability was defined as the initiation of compromise of the MoS_2's ability to provide low friction. Test durations were long enough to initiate this compromise. One-half of the gears tested had zero time exposure to humid air prior to testing. The other half of the gears were exposed to air of 57 percent relative humidity for exposure durations up to 77 days prior to testing.

On average the film durability was shorter for gears exposed to humid air compared to gears with zero exposure. The film durability for gears with zero exposure ranged from 190,300 to 53,300 pinion revolutions with an average value of 100,200 and a median value of 83,500 revolutions. The film

durability for gears exposed to humid air ranged from 84,700 to 21,000 pinion revolutions with an average value of 64,900 and a median value of 68,800 revolutions. Using the unexposed-gear film durability as a baseline, the exposure reduced the film durability by 35 percent based on average values or 18 percent based on median values. These reductions in film durability are similar magnitude compared to the 55 percent to 20 percent range of reductions reported by Lince, Loewenthal, and Clark [4].

The gear teeth had a very glossy appearance after very few revolutions of the gears. After this initial running-in, further change in the appearance of the teeth was a slow, steady process. Profilometry revealed that the wear depth at test completion was on the order of the specified MoS_2 film thickness.

Red-brown coloration was noted on some of the teeth that had been exposed to humid air. The colored regions appeared as soon as 17 days after exposure to humid air. SEM inspections showed that at least some of these colored areas included material raised above the surrounding MoS_2 film.

Acknowledgements

This research was supported by the NASA Engineering Safety Center (NESC). The experimental work was done with assistance from Tysen Mulder, NASA Pathways Intern. Dr. Iqbal Shareef was supported by the NASA GRC Summer Faculty Fellowship Program.

References

1. Gibson, A., et al, “Overview of Design and Validation of the Fine Guidance Sensor Mechanism for JWST”, 15th European Space Mechanisms and Tribology Symposium, vol. 718. 2013
2. Gibson, A. et al, "Life-test Investigation and Status of the NIRISS Dual Wheel Cryogenic Mechanism for JWST." 15th European Space Mechanisms and Tribology Symposium, vol. 718. 2013
3. Aldridge, D, et al, "Cryogenic Motor Enhancement for the NIRISS Instrument on the James Webb Space Telescope." ESA Special Publication, vol. 737. 2015.
4. Lince, J., Loewenthal, S. and Clark, C. “Degradation of Sputter-Deposited Nanocomposite MoS_2 Coatings for NIRCam during Storage in Air”, Proceedings of the 43rd Aerospace Mechanisms Symposium, (May, 2016) pp. 221-234, NASA/CP-2016-219090.
5. Krantz, Timothy, DellaCorte, C. and Dube, M., "Experimental Investigation of Forces Produced by Misaligned Steel Rollers." Proceedings of the 40th Aerospace Mechanisms Symposium, NASA/CP-2010-216272.
6. Krantz, T., and Shareef, I., "Wear of Steel and Ti6Al4V Rollers in Vacuum." Proceedings of the 41st Aerospace Mechanisms Symposium, NASA/CP-2012-21763.
7. Dellacorte, C., Krantz, T., and Dube, M., “ISS Solar Array Rotary Joint (SARJ) Bearing Failure and Recovery: Technical and Project Management Lessons Learned”, NASA/TP-2011-217116.
8. Pepper, S., “Research Note-Characterization of the Test Environment of JWST Roller Wear Evaluation at NASA-GRC”, Aug. 1, 2011.